Extraction of Alumina from the Coal Fly Ash by Hydrochloric Acid

Dmitry Valeev[1], Andrey Shoppert[2]
1. Senior researcher, IMET RAS, Moscow, Russia
2. Associate professor, Ural Federal University, Yekaterinburg, Russia
Correspondence author: dvaleev@imet.ac.ru

Abstract

Fly ash landfills that accumulate a by-product of coal combustion and gasification represent a permanent threat to the surrounding environment due to many factors (air and water pollution, soil contamination, wildlife poisoning, etc). Moreover, disposed coal fly ash may contain significant amounts of valuable elements that are not extracted. To improve the above situation, a combined ash treatment process was developed for utilisation of the coal fly ash waste from coal-fired power stations. The ash treatment includes three stages: 1) magnetic separation of an iron-containing fraction, 2) carbon separation by floatation, and 3) extraction of aluminum by the autoclave hydrochloric acid leaching. The lab-scale results of the ash treatment applied to the Ekibastuz brown coal fly ash from the Omsk power stations (Russia) were presented and discussed. The XRD analysis showed that the fly ash consists primarily of quartz, mullite and magnetite. It was found that the magnetic fraction separated at the first stage is enriched in magnetite (over 20 wt %), the carbon content in the concentrate after flotation increases to 27 wt %, and 90-95 % of aluminum can be extracted during the autoclave acid leaching. The SEM analysis showed that the magnetite phase is grown on the surface of aluminosilicate spheres as ~ 1 mm cubic crystals. The effect of the autoclave temperature and exposure time on the Al extraction efficiency was also investigated and analysed in the present paper. The optimal autoclave temperature and exposure time were found to achieve the maximum Al extraction efficiency. It was also found by the SEM microanalysis that further extraction of aluminum is not economically feasible since the remaining Al is evenly surrounded by SiO_2 in the fly ash particles.

Keywords: coal fly ash, magnetic separation, flotation, leaching, hydrochloric acid.

1. Introduction

A lot of power stations world-wide still use coal combustion as a main process to generate electricity and heat. In the city of Omsk thermal power stations utilize brown coal from the Ekibastuz coal field (Kazakhstan), which is characterised by high ash content (up to 40 %) [1]. Electricity and heat for the Omsk city is produced mainly by two coal-fired power stations TPS-4 and TPS-5 that generate 450 000 and 1 150 000 tons of coal fly ash (CFA) per year, respectively. In total, ash disposal sites near Omsk accumulate more than 75 billion tons of CFA [2].

CFA usually contains from 20 to 35 wt % of Al_2O_3, which can partially be extracted by different methods [3,4]. Recent studies on the Al extraction from CFA using acid leaching show that hydrochloric acid is the most reactive in regard to Al compared to sulphuric, nitric and hydrofluoric acids [5]. However, if leaching is carried out at atmospheric pressure (e.g. 6M HCl, T = 107 °C) the extent of Al extraction does not exceed 70 % [6,7] One of the most perspective methods to intensify leaching of a high-silica aluminum-containing feedstock is to use autoclaves [8,9]. This method allows to exclude preliminary annealing and two-stage leaching. As silicon dioxide does not react with acids a preliminary desilication is not necessary. Besides aluminum iron will also go into the solution, which makes it necessary first to remove magnetite by magnetic separation.

In the present work a combined treatment of the raw CFA collected from the Omsk TPS-4 was carried out in three stages: 1) iron separation by magnetic separation, 2) carbon separation by floatation, and 3) aluminum extraction by autoclave acid leaching.

2. Experimental

The raw CFA collected from the Omsk TPS-4 ash disposal site (that contains ~37 billion ton of fly ash) was used as an initial waste material. The CFA is produced from combustion of the Ekibastuz brown coal (Kazakhstan) on the Omsk TPS-4. The average chemical composition of the raw CFA is given in Table 1.

Table 1. The average chemical composition [wt. %] of CFA from TPS-4 (Omsk, Russia).

Component	SiO_2	Al_2O_3	Fe_2O_3	TiO_2	K_2O	CaO	MgO	MnO	Na_2O	P_2O_5	LOI*
Contents	59.66	24.26	5.42	1.15	0.74	0.88	0.40	0.11	0.44	0.45	6.49

*LOI – loss on ignition at 1000 °C

A roll-type magnetic separator MBS 150x125 (NPO “Erga”, Russia) was used to separate the magnetic and non-magnetic fractions of CFA. Initial CFA samples of ~500 g were mixed with water and loaded into the separator. The magnetic field strength applied was 110 mT.

Carbon flotation tests were carried out in a flotation machine 189FL (REC “Mekhanobr-Tekhnika”, Russia) using methyl isobutyl carbinol (MIBC) as a foamer (frother) and kerosene KO-25 as a collector. Typical CFA amount and water volume were 20 g and 100 ml, respectively.

The flotation efficiency index commonly used in mineral processing was employed as an efficiency criterion:

$$E = [(\varepsilon - \gamma) / (100 - \alpha)] \times \cdot 100\% \qquad (1)$$

where ε is the percentage of carbon/sulphur extraction from the non-magnetic fraction; γ is the amount of the carbon/sulphur concentrate relative to the initial mass of the non-magnetic fraction; α is the carbon/sulphur content in the CFA non-magnetic fraction.

Leaching of coal fly ash by hydrochloric acid to extract aluminum was carried out in a laboratory autoclave using stainless steel capsules with 50 ml Teflon inserts (Deschem, China). The autoclave temperature was governed by a PID controller with ±1°C accuracy. The heating time from room temperature up to a particular temperature was approximately 1 hour. The exposure times at different temperatures (160, 170, 180, 190, 200°C) were 1, 2, 3, 4 hours, respectively. The HCl concentration was 345 g/l (30 %); the ratio S:L = 1:5.

3. Results and Discussion

Figure 1 showed the XRD results of the initial CFA (TPS-4, Omsk, Russia), and the magnetic & non-magnetic fractions after the wet magnetic separation. It can be seen that the initial CFA consists mainly of mullite, quartz and magnetite. In general, the mullite phase is a non-stoichiometric solid solution between SiO_2 and Al_2O_3 with an approximate formula $Al_6Si_2O_{13}$. The quartz and magnetite phases have stoichiometric formulae SiO_2 and Fe_3O_4, respectively; however, while quartz is a SiO_2 polymorph, magnetite generally represents a solid solution between FeO and Fe_2O_3 with a spinel-type structure that can accommodate other atoms like Ca, Mg and Mn.

The wet magnetic separation tests demonstrate that the magnetic fraction can consist up to 10% of the initial fly ash mass. The magnetite content in the magnetic fraction after separation increases from 5 to 20 wt. %. The non-magnetic fraction contains less than 1 wt. % of iron oxide, and the Al_2O_3 amount increases from 24 to 27 wt. % (Table 2). It can be seen that Ca, Mg, Mn, P occur mainly in the magnetic fraction, while Ti and C are present in the non-magnetic fraction.

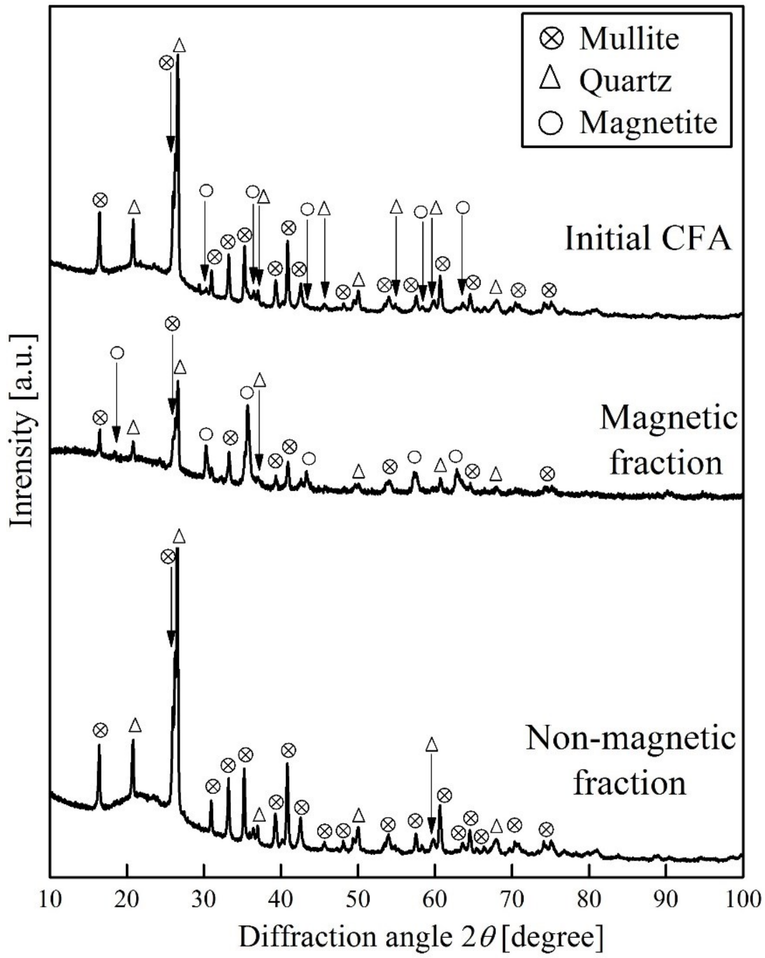

Figure 1. XRD patterns of the initial CFA and the magnetic & non-magnetic fractions after the wet magnetic separation.

Table 2. The bulk chemical composition [wt. %] of the magnetic & non-magnetic fractions after the wet magnetic separation of CFA from TPS-4, Omsk, Russia.

Component	SiO_2	Al_2O_3	Fe_2O_3	TiO_2	K_2O	CaO	MgO	MnO	Na_2O	P_2O_5	LOI
Magnetic fraction	55.94	14.73	20.2	0.75	0.4	1.28	0.66	0.67	0.28	0.64	4.45
Non-magnetic fraction	62.89	27.01	0.63	1.33	0.35	0.09	0.14	0.18	0.32	0.42	6.77

*LOI – loss on ignition at 1000 °C

Morphology of ash particles from the magnetic and non-magnetic fractions obtained by SEM is shown in Figures 2(a-b), while the corresponding elemental spectra are given in Table 3. The magnetic fraction consists primarily of spherical particles of 30-60 µm, with small cubic crystals (about 1 µm) of magnetite grown on their surface. The amount of magnetite on the particles surface is not significant compared to the alumosilicate content, which implies that the magnetite concentration in the magnetic fraction cannot be increased to 50-75 %. The non-magnetic fraction consists of agglomerates of irregular shape with a size of 20-80 µm.

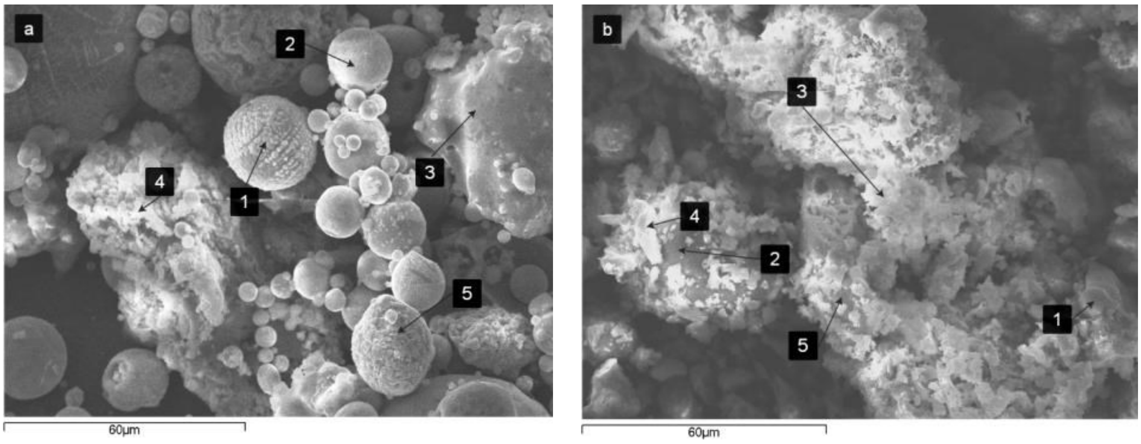

Figure 2. Typical SEM images of the magnetic (a) and non-magnetic fractions (b).

Table 3. The elemental compositions [at. %] of particles from the magnetic and non-magnetic fractions (see Figure 2 for the spectra numbers).

Spectrum	O	Na	Mg	Al	Si	Ca	Ti	Fe
Magnetic fraction								
1	69.40	-	1.47	1.04	5.72	0.62	-	21.75
2	65.53	-	-	0.55	1.17	0.70	-	32.05
3	50.92	-	-	-	10.29	-	-	38.79
4	75.07	-	0.20	3.71	19.8	-	-	1.22
5	63.52	-	1.82	1.90	3.80	0.53	-	28.43
Non-magnetic fraction								
1	72.99	-	-	8.97	15.98	0.57	0.37	1.11
2	63.35	-	1.05	4.34	20.21	2.79	6.30	1.96
3	74.16	-	-	5.02	20.82	-	-	-
4	74.35	0.27	0.43	10.80	13.54	0.35	-	0.27
5	59.77	-	-	17.35	22.88	-	-	-

The non-magnetic fraction obtained after the wet magnetic separation contains about 6.5 wt. % of carbon and 0.04 wt. % of sulphur. It was screened into size fractions from 40 to 400 µm, and the C and S concentrations was determined for each size fraction (Table 4).

It can be seen from Table 4 that CFA particles over 100 µm contain 10-30 wt. % of carbon and 0.07-0.24 wt. % of sulphur. CFA particle size distribution and carbon content agree with the reported data by Bartoňová [10]. Figure 3 shows porous spherical particles that contain most carbon present in fly ash [11]. It can be seen that the average size of those particles is bigger than 200 µm.

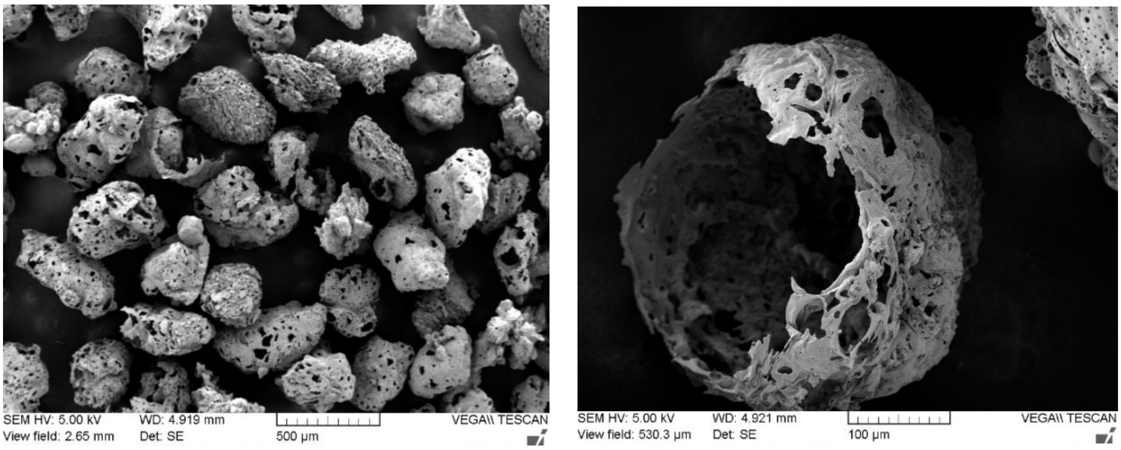

Figure 3. The SEM images of carbon particles from the CFA non-magnetic fraction.

Table 4. The carbon and sulphur concentrations in the non-magnetic fraction as a function of the particle size.

Particle size, μm	Fraction in CFA, %	Carbon content, wt. %	Sulphur content, wt. %
315-400	0.28	30.9	0.242
200-315	1.65	25.6	0.179
160-200	1.78	18.5	0.128
100-160	17.88	9.96	0.069
71-100	15.46	7.14	0.053
63-71	19.33	5.57	0.041
40-63	18.59	3.72	0.029
40 <	25.02	2.27	0.023

It was found [12] that the most suitable particle size for flotation should lie in a range of 40-71 μm. Therefore, the ash fraction that contains particles over 71 μm was subjected to grinding. The obtained carbon-enriched concentrate was processed by flotation. Kerosene was chosen as the collector in flotation due to its effectiveness and cheap price [13].

The results of flotation tests are shown in Figures 4(a - d), which represent the efficiency index *E* (calculated by Equation 1 for carbon and sulphur) as a function of the collector volume for (a-b) small particles (40 - 71 μm) processed by flotation and (c - d) large particles (100 - 400 μm) first grinded to 40 - 71 μm and then processed by flotation. It can be seen that the efficiency index for carbon increases to ~ 67.8 % as the collector volume changed from 0.5 to 1.5 ml. Further increase of the collector volume to 2 ml decreases the *E* index to 51 % (Figure 4a). As the large-size (100 - 400 μm) ash fraction contains significantly more carbon than the small-size fraction (< 100 μm), the collector volume was increased; the best efficiency was achieved on adding 5 ml of kerosene (Figure 4(c)). However, as in the case of small-size fraction, an increase of the collector volume to 7.5 ml decreases the flotation efficiency index to 32 %, because the larger the collector volume, the greater the amount of alumosilicate particles collected in flotation. It can be seen from Figures 4(b, d) that similar trends were observed for sulphur flotation, but poorer flotation efficiency indices can be achieved than those for carbon (the corresponding values are 54 and 33.8 %).

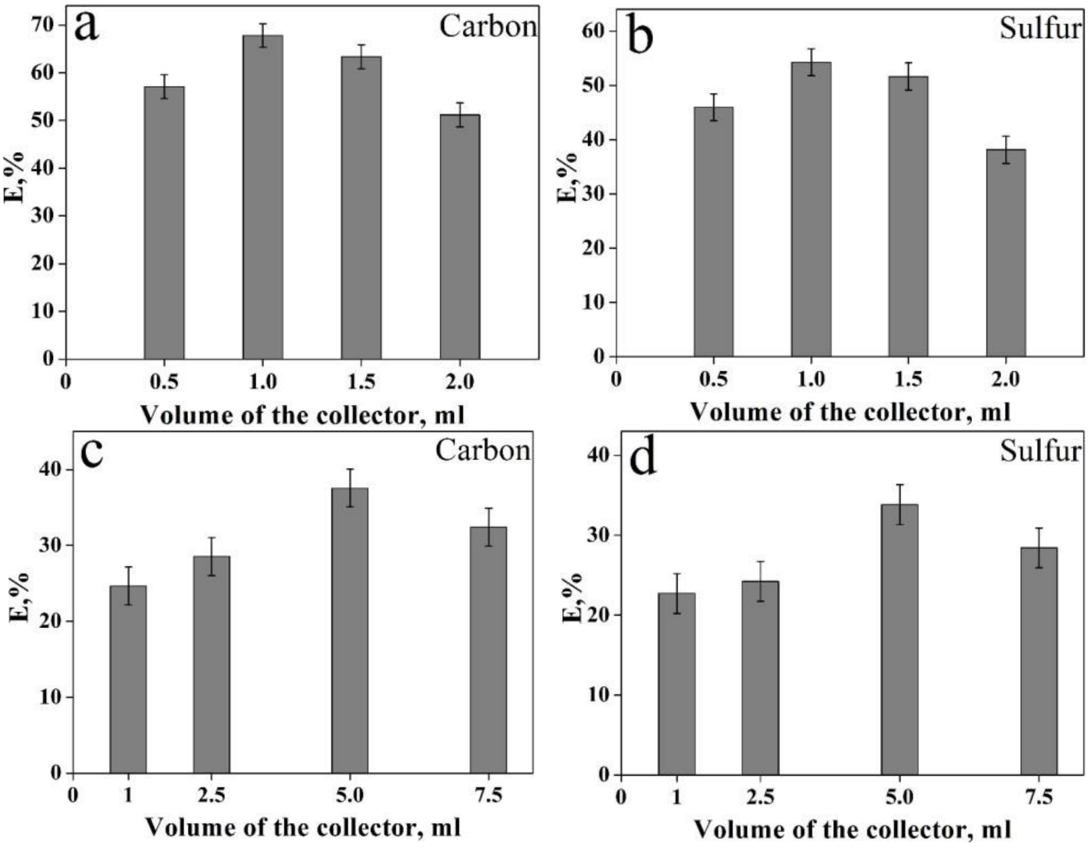

Figure 4. The effect of the collector volume on the flotation efficiency index *E*: (a–b) for CFA particles of 40-71 µm after screening non-magnetic fraction carbon; (c–d) for CFA particles of 100-400 µm after grinding to 40-71 µm.

Aluminum is mainly present in CFA as mullite. A reaction between mullite and hydrochloric acid (6M) at a boiling temperature results in extraction of maximum 15 % of aluminum. Fluorides of alkali and alkaline earth metals (KF, NaF, CaF_2) as well as ammonium fluoride (NH_4F) are usually added to intensify the Al extraction. Fluoride reacts with SiO_2 and destroys the Si-Al bond, forming SiF_4, which hydrolyses with formation of H_2SiF_6 [14]. This method leads to a substantial increase of the Al extraction efficiency, up to 90-95 % [15]. However, possible formation of hydrofluoric acid during such treatment restricts the final product, aluminum chloride solution to be further used as a coagulant for water purification [16]. Therefore, in the present work an autoclave leaching technique was used to enhance the efficiency of Al extraction instead the fluoride addition method. The XRD analysis of the non-magnetic fraction showed only the presence of quartz and mullite (Figure 1), which implies that the Al extraction process can roughly be represented by the following reaction between hydrochloric acid and stoichiometric mullite:

$$3Al_2O_3 \cdot 2SiO_{2(s)} + 18HCl_{(l)} = 6AlCl_{3(aq)} + 2SiO_{2(s)} + 9H_2O_{(l)} \qquad (2)$$

The effect of the autoclave temperature and exposure time on the Al extraction efficiency is shown in Figure 5. It can be seen that an increase of the autoclave temperature leads to an increase of the Al extraction efficiency. The greatest extraction efficiency of 90 – 95 % was observed at temperatures 190 – 200 °C after ~3 hours of leaching. The chemical composition of the solution obtained at T = 200 °C and τ = 3 hours is as follows [g/l]: Al – 23.6, Fe – 2.1, K – 0.9, Mg – 0.3, Na – 0.6, Ti – 0.6, Sc – 0.002.

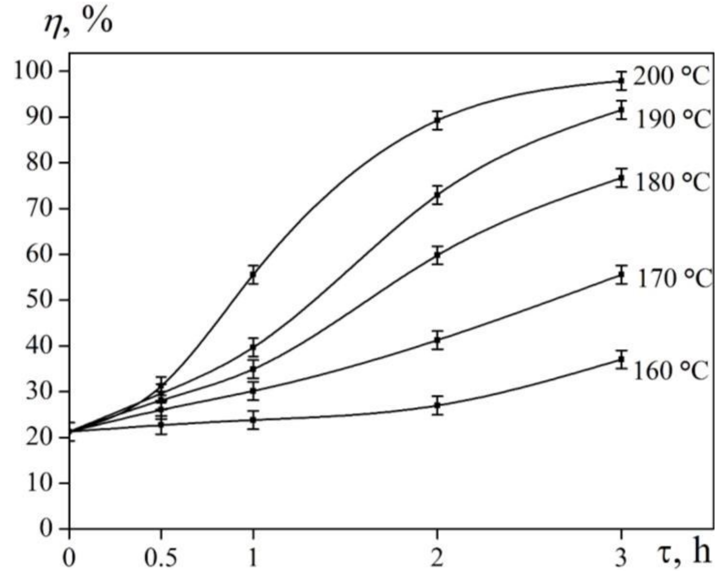

Figure 5. The effect of the autoclave temperature and exposure time on the Al extraction efficiency (the solid lines are drawn for eye guidance).

The solid residue that is filtrated after leaching consists mainly of SiO_2 (Table 5) with small amounts of C, Al_2O_3 and TiO_2. The XRD analysis shows the presence of quartz and residual mullite (Figure 6).

Table 5. The average chemical composition [wt. %] of the solid residue after autoclave leaching of CFA by hydrochloric acid at T = 200 °C, S:L = 1:5, τ = 3 hours.

Component	SiO_2	Al_2O_3	Fe_2O_3	TiO_2	K_2O	CaO	MgO	MnO	Na_2O	P_2O_5	LOI*
Contents	92.05	3.61	0.12	1.67	0.4	0.34	0.07	0.03	0.23	0.46	1.02

*LOI – loss on ignition

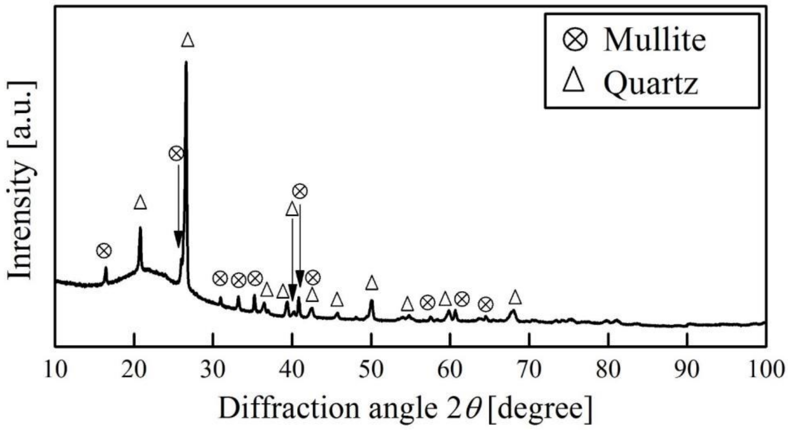

Figure 6. XRD pattern of the solid residue after autoclave leaching of CFA by HCl at T = 200 °C, S:L = 1:5, τ = 3 hours.

This solid residue can further be utilised in ceramic (SiC) manufacturing [17] or as an addition to Portland cement to increase its toughness [18].

The Al extraction process by acid leaching can be described as a reaction rate process with a thermally activated reaction rate constant. The activation energy for hydrochloric acid leaching of mullite can then be determined from the Arrhenius equation for the reaction rate constant *k*:

$$k = A \cdot \exp(-E_a / RT) \qquad (3)$$

where A is the pre-exponential term; E_a is the activation energy; R is the universal gas constant.

Figure 7 shows the logarithm of the reaction rate constant as a function of reciprocal temperature constructed on the basis of the experimental data (Figure 5). The activation energy was determined as a tangent to a linear curve “ln*k* vs T^{-1}”. It can be concluded from the obtained value of E_a (55.5 kJ/mol) that the mullite leaching process can be limited by the corresponding chemical reaction kinetics, not by diffusion, because $E_a > 40$ kJ/mol [19].

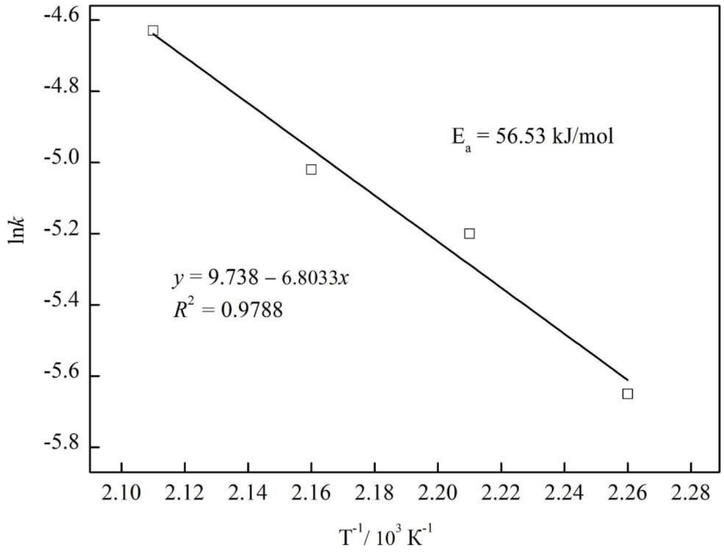

Figure 7. The logarithm of the reaction rate constant as a function of reciprocal temperature during the autoclave leaching process.

These research were carried out in a laboratory setup, where the agitation practically had no effect on the leaching process. The obtained experimental data will be used in further investigations using a 5 l glass lined high-pressure reactor with a stirrer. Since the industrial application of such equipment involves work at T = 150 – 180 °C, we will focus on these indicators. A potential method of intensifying the leaching process can be used pretreatment of ash by alkali to dissolve part of the silica into the solution and destroy the surface layer of ash particles. This will lead to a better interaction of mullite by hydrochloric acid [20]. The use of 30 % HCl in this research is due to the orientation of this study on coagulant production. When studying the method of alumina production, it is necessary to reduce the concentration to 20 % in order to reuse during the pyrohydrolysis of aluminum chloride hexahydrate.

4. Conclusions

Combined treatment to utilise the coal fly ash waste collected from the Omsk TPS-4 (Russia) was developed, lab-scale tested and analysed. Three-stage treatment includes magnetic separation of iron-containing fraction, carbon separation by flotation and aluminum extraction by autoclave acid leaching.

The magnetite amount in the magnetic fraction after separation increases from 5.3 to 20.2 wt. %, while the Al_2O_3 amount in the non-magnetic fraction increases from 24.5 to 27 wt. %. The carbon content in the concentrate obtained after flotation using kerosene as the collector reaches ~27 wt. %.

The effect of the autoclave temperature and exposure time on the aluminum extraction efficiency was investigated for the autoclave hydrochloric acid leaching process. The Al extraction efficiency can reach ~95 % at the following optimal process parameters: T = 200 °C, C_{HCl} = 345 g/l, τ = 3 h, S:L = 1:5. The activation energy of the leaching process determined from the experimental data was 56.5 kJ/mol, which means that the process limiting stage is probably surface chemical reaction.

5. Acknowledgements

The present study was funded by the Russian Science Foundation project No 18-79-00305.

6. References

1. B. Dikhanbaev et al., Development of hydrogen-enriched water gas production technology by processing ekibastuz coal with technogenic waste, *Arch. Mech. Eng*. V. 65, (2018), 221-231.
2. V.V. Sirotyuk et. al., Strength and deformation characteristics of ash and slag mixture, *Mag. Civ. Eng*. V. 74, (2017), 1-14.
3. J. Ding et al., Research and industrialization progress of recovering alumina from fly ash: A concise review, *Waste Manag*. V. 60, (2017), 375-387.
4. P.K. Sahoo et al., Recovery of metals and other beneficial products from coal fly ash: a sustainable approach for fly ash management, *Int. J. Coal Sci. Technol*. V. 3, (2016), 267-283.
5. P. Hu et al., Distribution and occurrence of lithium in high-alumina-coal fly ash, *Int. J. Coal Geol.* V. 189, (2018), 27-34.
6. R. Singh et al., Beneficiation of iron and aluminium oxides from fly ash at lab scale, *Int. J. Miner. Process.* V. 145, (2015), 32-37.
7. Q. Luo et al., Dissolution Kinetics of Aluminum, Calcium, and Iron from Circulating Fluidized Bed Combustion Fly Ash with Hydrochloric Acid, *Ind. Eng. Chem. Res.* V. 52, (2013), 18184-18191.
8. C.Y. Wu et al., Extraction of aluminum by pressure acid-leaching method from coal fly ash, *Trans. Nonferrous Met. Soc. China* V. 22, (2012), 2282-2288.
9. J. Xiao et al., Co-utilization of spent pot-lining and coal gangue by hydrothermal acid-leaching method to prepare silicon carbide powder*, J. Clean. Prod.* V. 204, (2018), 848-860.
10. L. Bartoňová, Unburned carbon from coal combustion ash: An overview, *Fuel Process. Technol.* V. 134, (2015), 136-158.
11. J.C. Hower et al., Coal-derived unburned carbons in fly ash: A review, *Int. J. Coal Geol.* V. 179, (2017), 11-27.
12. Y.V. Ryabov et al., PAV-2 conditioning agent application efficiency in flotation of unburned carbon from coal-fired power plants fly ash, *Obogashchenie Rud*. (2018), 43-49.
13. G. Han et al., Enhanced recycling and utilization of mullite from coal fly ash with a flotation and metallurgy process*, J. Clean. Prod.* V. 178, (2018), 804-813.
14. J. Li, et al., Acid leaching aluminum from boiler slag - Effect of fluoride additives on the aluminum dissolution, *Appl. Mech. Mater.* V. 71-78, (2011), 688-693.
15. A.K. Tripathyet al., Aluminium recovery from NALCO fly ash by acid digestion in the presence of fluoride ion, *Int. J. Miner. Process.* V. 138, (2015), 44-48.
16. K. Hu et al., Preparation of an Aluminum and Iron-Based Coagulant from Fly Ash for Industrial Wastewater Treatment, *Clean - Soil, Air, Water.* V. 45 (9), (2017), 1600437
17. F. Li et al., Preparation of SiC from acid-leached coal gangue by carbothermal reduction, *Int. J. Appl. Ceram. Technol.* V. 15, (2018), 625-632.

18. Y. Reches et al., Agglomeration and reactivity of nanoparticles of SiO_2, TiO_2, Al_2O_3, Fe_2O_3, and clays in cement pastes and effects on compressive strength at ambient and elevated temperatures, *Constr. Build. Mater.* V. 167, (2018), 860-873.
19. L. Tian et al., Kinetics of indium dissolution from marmatite with high indium content in pressure acid leaching, *Rare Met.* V. 36, (2017), 69-76.
20. Z. Ma et al., Novel extraction of valuable metals from circulating fluidized bed-derived high-alumina fly ash by acid–alkali–based alternate method, *J. Clean. Prod.* V. 230, (2019), 302-313.